Proceedings of the Seventh International Conference on
Railway Technology: Research, Development and Maintenance
Edited by: J. Pombo
Civil-Comp Conferences, Volume 15, Paper 18.4
Civil-Comp Press, Edinburgh, United Kingdom, 2026
ISSN: 2753-3239, doi: 10.4203/ccc.15.18.4
©Civil-Comp Ltd, Edinburgh, UK, 2026

Effect of Crosswinds on Flange Climb Derailment in Curved Sections Without Anti-Derailment Guards

S. Kishiya and H. Kanemoto

Railway Technical Research Institute, Japan

Abstract

Ensuring the stability of railway vehicles under hazardous conditions such as strong crosswinds is critical for maintaining operational safety and reliability. Among the various countermeasures, anti-derailment guards play an important role in reducing the risk of flange climb derailment. Current installation standards for these guards are primarily determined quantitatively based on the estimated derailment coefficient ratio in Japan. However, these standards do not incorporate the influence of crosswinds, which can significantly alter wheel–rail interaction and increase derailment risk. This study evaluates the effects of crosswinds on flange climb derailments in curved track sections where the estimated derailment coefficient ratio slightly exceeds 1.2—just short of meeting the derailment guard installation standards—to investigate the impact of crosswinds on these installation standards. To achieve this, we conduct simulations using a multibody dynamics model that replicates running tests under crosswind conditions. The results confirmed that the derailment coefficient on the outer rail side of the curve increased, and that the wheel contact point shifted closer to the flange position. These findings indicate that installing anti-derailment guards is important in strong crosswind environments, particularly under track conditions where the estimated derailment coefficient ratio slightly exceeds 1.2.

Keywords: flange climb derailment, anti-derailment guards, crosswinds, simulations, multibody dynamics, estimated derailment coefficient ratio, curve radius, cant amount, cant gradient, running speed.

1 Introduction

Regarding the effect of crosswinds on the running safety of railway vehicles, overturning accidents have mainly been a concern. Previous research has primarily focused on improving the accuracy of evaluating wind speeds at which overturning occurs. Since derailments caused by crosswinds can result in catastrophic damage once they occur, the importance of this research is expected to remain unchanged.

On the other hand, crosswinds may also influence flange climb derailments. In curved sections, winds blowing from the outer rail toward the inner rail can reduce the vertical contact force on the outer rail, potentially increasing the derailment coefficient compared to calm conditions. However, there are few existing research examples or accident reports indicating crosswinds have influenced flange climb derailments. This is largely because wind speed data is generally unavailable at accident sites, making it difficult to quantitatively assess crosswind effects. Furthermore, considering the recent trend toward lighter vehicles, which are more susceptible to crosswind effects, the impact of crosswinds on both capsizes and flange climb derailment deserves attention as a critical factor for future operational safety and reliability.

Among the countermeasures to maintain operational safety and reliability, anti-derailment guards play a crucial role in reducing the risk of derailment due to flange climb derailment. The installation standards for anti-derailment guards are currently determined quantitatively based on the estimated derailment coefficient ratio [1] value calculated using parameters such as curve radius, cant amount, and cant gradient in Japan. However, no standards have been established that consider the influence of crosswinds. In this study, we evaluate the effects of crosswinds on flange climb derailment in curved track sections where the estimated derailment coefficient ratio slightly exceeds 1.2—just below the threshold for requiring anti-derailment guard installation standards—to clarify how crosswinds influence the applicability of these installation standards.

2 Methods

This section describes the multibody dynamics (MBD) model used to calculate wheel–rail contact forces under crosswind conditions and the evaluation method for estimated derailment coefficient ratio to extract curve conditions such as curve radius, cant amount, and cant gradient near the installation threshold for anti-derailment guards.

2.1 Multibody dynamics model

The MBD model used in this study is shown in Figure 1, created using the simulation software SIMPACK. The bogie is modelled based on a standard bolsterless bogie. Each bogie is equipped with lateral dampers but no vertical dampers. The carbody length is approximately 20 m. Based on previous research that conducted wind tunnel tests using a 1/10 scale vehicle model to investigate the effects of vertical contact force and lateral contact force changes due to crosswinds on flange climb derailment [3], the vehicle specifications of the 1/10 scale model is converted to values equivalent to the actual vehicle and applied to the MBD model. The main vehicle specifications converted from the 1/10 scale vehicle model applied to the MBD model are shown in Table 1.

In this study, we investigated the effects of crosswinds blowing from the outer track toward the inner track while running through a left curve, as shown in Figure 1. Note that the curve radius, cant amount, and cant gradient for this left curve were set as parameters where an anti-derailment guard could barely be installed.

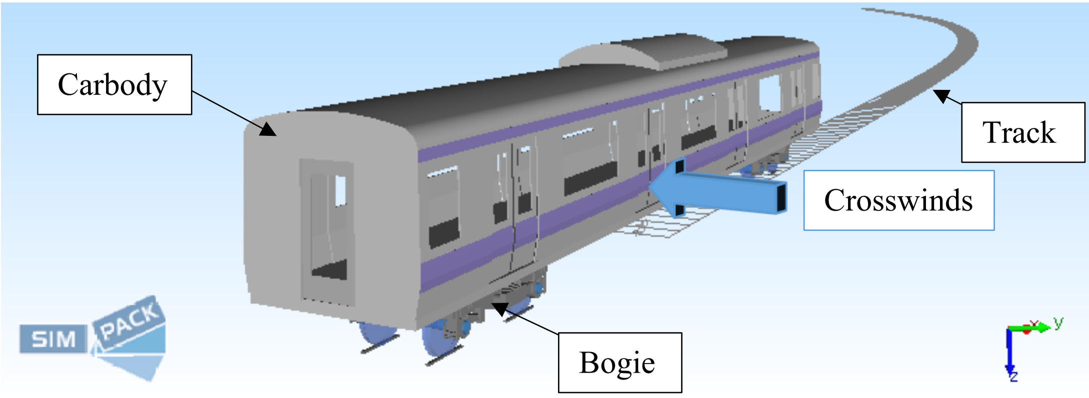

Figure 1: MBD model.

Category	Value
Carbody mass [kg]	14640
Bogie mass [kg]	5295
Carbody center of gravity height [m]	2.14
Center height of carbody [m]	2.36
Carbody height [m]	2.63
Side area of the carbody [m^2]	51.29
Track gauge [m]	1.067

Table 1: The main specifications of the MBD model.

2.2 Estimated derailment coefficient ratio

To investigate the effect of crosswinds leading to flange climb derailment on curves where the installation standards for anti-derailment guards are barely fulfilled, an estimated derailment coefficient ratio $(Y/Q)_{ratio}$ [1] is used. The estimated derailment coefficient ratio is given by the following Equation (1).

$$(Y/Q)_{\text{ratio}} = \frac{(Y/Q)_{\text{cri}}}{(Y/Q)_{\text{est}}} \tag{1}$$

Here, Y is lateral contact force, Q is vertical contact force. $(Y/Q)_{\text{est}}$ denotes the estimated derailment coefficient calculated as the ratio of the estimated lateral contact force Y_{est} and the estimated vertical contact force Q_{est}. During this process, Y_{est} is calculated considering factors such as the friction coefficient, unbalanced centrifugal force, and the yaw resistance of the bogie. Q_{est} is calculated considering factors such as unbalanced centrifugal force and track twist. $(Y/Q)_{\text{cri}}$ is calculated from Nadal's equation, which is used to quantitatively calculate the margin against flange climb derailment, as shown in Equation (2).

$$(Y/Q)_{\text{cri}} = \frac{\tan\alpha - \mu_e}{1 + \mu_e \tan\alpha} \tag{2}$$

$$\mu_e = \frac{27.0\times\alpha}{\left\{\mu^{1.5} + (27.0\times\alpha)^{1.5}\right\}^{\frac{2}{3}}}\mu \tag{3}$$

Here, μ_e is equivalent friction coefficient, α is wheel flange angle and μ is dynamic friction coefficient. Note that α is set to the standard flange angle for conventional lines, and μ is set to 0.3. The installation standard for anti-derailment guard requires installation when $(Y/Q)_{\text{ratio}} < 1.2$, whereas installation is not required when $(Y/Q)_{\text{ratio}} \geqq 1.2$ [2].

The combinations of curve radius R, cant amount e, and cant gradient l that barely achieve $(Y/Q)_{ratio} \geqq 1.2$ are shown in Table 2. Note that $(Y/Q)_{ratio}$ is calculated using the specifications shown in Table 1 and parameters such as α, μ_e, R, e, and l.

R [m]	e [mm]	l [-]	$(Y/Q)_{ratio}$
300	60	450	1.24
300	70	650	1.22
400	80	500	1.23
400	90	600	1.23
500	105	400	1.28

Table 2: Combinations of curve radius, cant amount, and cant gradient that barely achieve $(Y/Q)_{ratio} \geqq 1.2$.

The combinations of R, e, and l shown in Table 2 are applied to SIMPACK's track conditions to examine their effect on flange climb derailment while running on a curve under crosswind conditions.

3 Results

To verify the accuracy of the constructed MBD model, we compare the vertical contact force, lateral force, and derailment coefficient obtained from the MBD model during passing curves under crosswinds, wind tunnel tests using a 1/10 scale vehicle model, and estimated crosswind-induced vertical contact force and lateral force formula [3]. Since the curve radius is 10 m and cant amount is 10.5 mm for the 1/10 scale vehicle model, the curve radius for the MBD model's curve radius should be 100 m and the cant amount should be 105 mm based on the similarity principle. Figure 2 shows the outer rail side vertical contact force Q_o, outer rail side lateral pressure Y_o, and outer rail side derailment coefficient Y_o / Q_o for the front bogie's front axle with varying running speed v and crosswind speed w. Note that the plots are based on a 1/10 scale vehicle model, solid lines represent the MBD model, and dashed lines indicate the estimated crosswind-induced vertical contact force and lateral force formula. Moreover, the MBD model's values for v, w, Q_o, Y_o, and Y_o / Q_o are scaled down to correspond to the 1/10 scale vehicle model based on the similarity principle. Y_o / Q_o obtained from the MBD model was selected at the point showing the highest value during curve passage under crosswind conditions, and the corresponding Q_o and Y_o are shown in Figure 2. Q_o, Y_o, and Y_o / Q_o calculated using the estimated crosswind-induced vertical contact force and lateral force formula showed relatively large estimation errors compared to the wind tunnel test results of the 1/10 scale vehicle model. However, using the MBD model improved the error in all cases. Also, with increasing w, the tendency of reduced Q_o, reduced Y_o and increased Y_o / Q_o observed in wind tunnel tests on 1/10 scale vehicle models is replicable using the estimated crosswind-induced vertical contact force and lateral force formula and the MBD model. Furthermore, wind tunnel test results for 1/10 scale vehicle models indicate that the speed dependence of Y_o, Q_o, and Y_o / Q_o is relatively small. This trend is also reproduced in the estimated crosswind-induced vertical contact force and lateral force formula and the MBD model. As a result of comparing the wind tunnel test results using a 1/10 scale vehicle model to verify the accuracy of the constructed MBD model, Q_o, Y_o, and Y_o / Q_o were generally consistent.

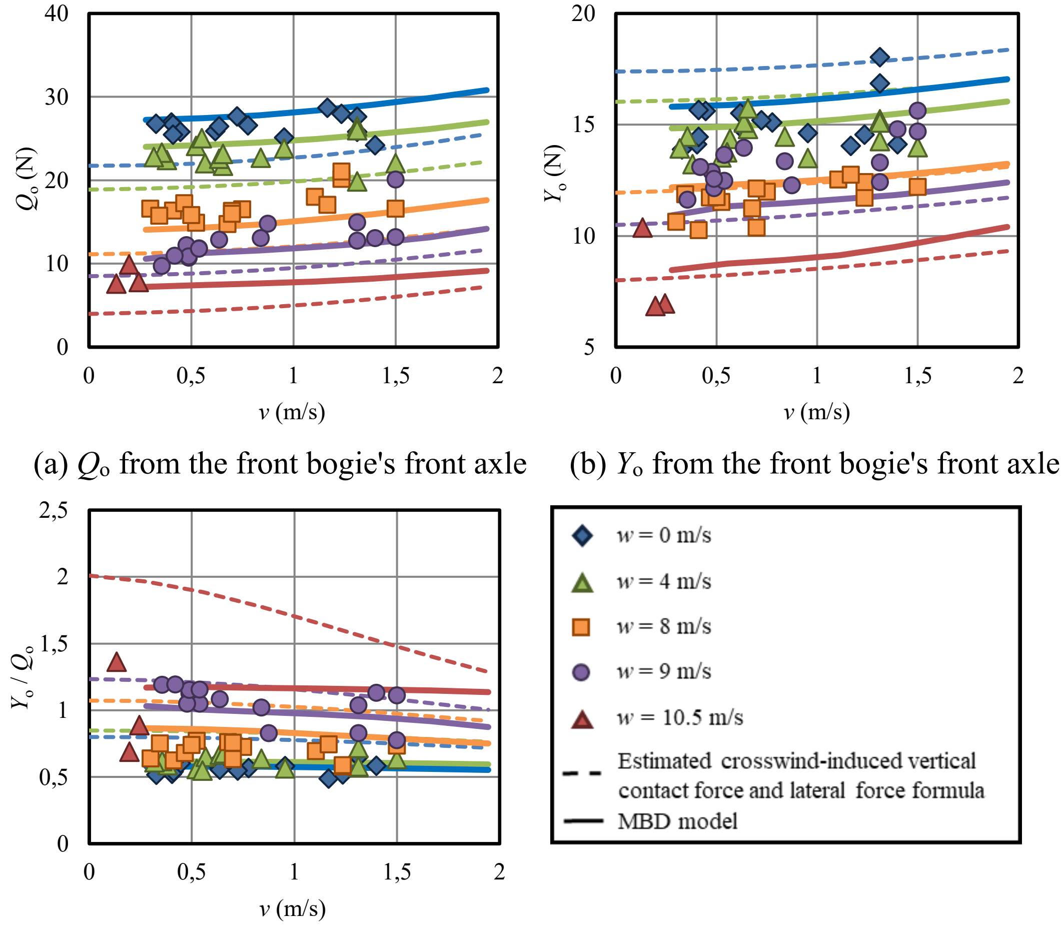

(a) Q_o from the front bogie's front axle (b) Y_o from the front bogie's front axle

(c) Y_o / Q_o from the front bogie's front axle

Figure 2: Variation of vertical contact force, lateral pressure, and derailment coefficient as a function of running speed.

We will verify the effect of crosswinds on derailment while running through the curve section shown in Table 2 at w = 0 m/s and 25.0 m/s using the validated MBD model. w = 25.0 m/s were selected based on the wind speed regulatory value widely adopted for railway operations in Japan, as train operations are suspended or restricted as a safety measure when w exceed this level. Figures 3 to 5 show the Q_o, Y_o, and Y_o / Q_o in relation to v at w = 0 m/s and 25.0 m/s. Figure 6 shows the difference Y_o / Q_o between w = 0 m/s and w = 25.0 m/s. In Figure 3, regardless of v, w, e, or l, Q_o tends to decrease as R increases. In Figure 4, similarly to Q_o, Y_o decreases with increasing R at any v, w, e, or l. Furthermore, while Y_o decreases when crosswinds occur, the rate of decrease tends to become smaller as the R increases. From Figure 5, it can be confirmed that at w = 0 m/s, Y_o / Q_o decreases as R increases, regardless of v, e, or l. However, at w = 25 m/s, Y_o / Q_o increases as R increases. Figure 6 shows that as R increases, the difference in Y_o / Q_o between w = 0 m/s and w = 25.0 m/s becomes larger. Additionally, as v increases, the difference in Y_o / Q_o tends to gradually decrease regardless of R. This is because Y_o / Q_o at w = 25.0 m/s in Figure 5 shows a tendency to gradually decrease. It is considered that this gradual decrease in Y_o / Q_o occurred because the centrifugal force acting on the car body increases with rising v, counteracting the aerodynamic force resulting in Q_o increasing.

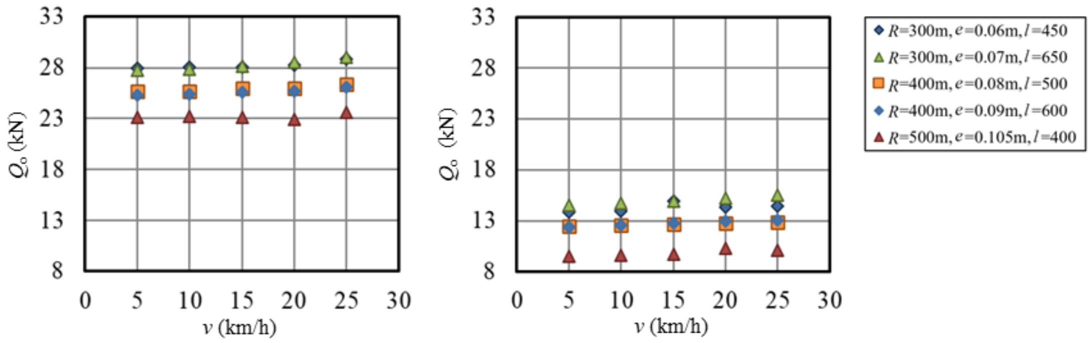

(a) w = 0 m/s (b) w = 25.0 m/s

Figure 3: Variation of vertical contact force as a function of running speed.

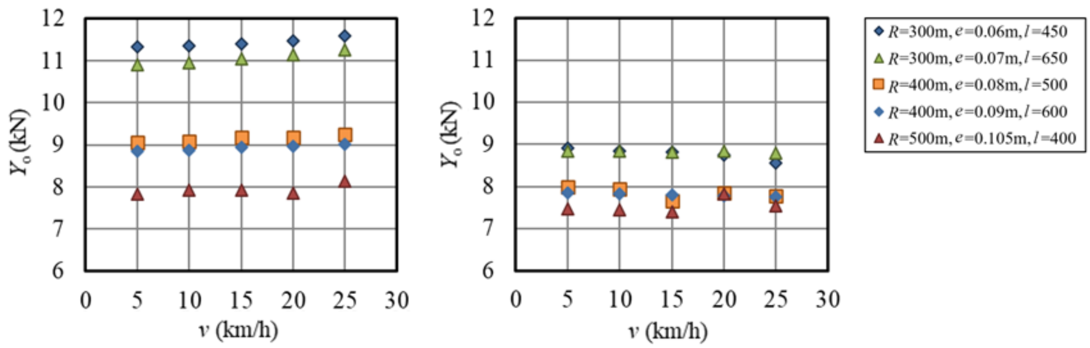

(a) w = 0 m/s (b) w = 25.0 m/s

Figure 4: Variation of lateral pressure as a function of running speed.

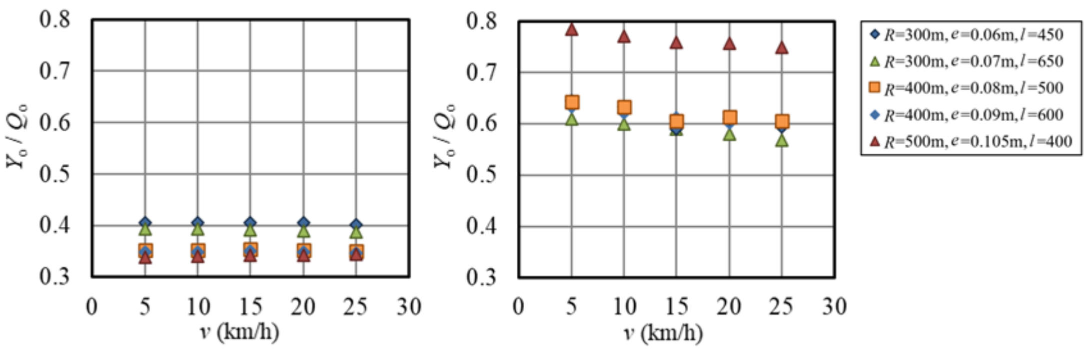

(a) w = 0 m/s (b) w = 25.0 m/s

Figure 5: Variation of derailment coefficient as a function of running speed.

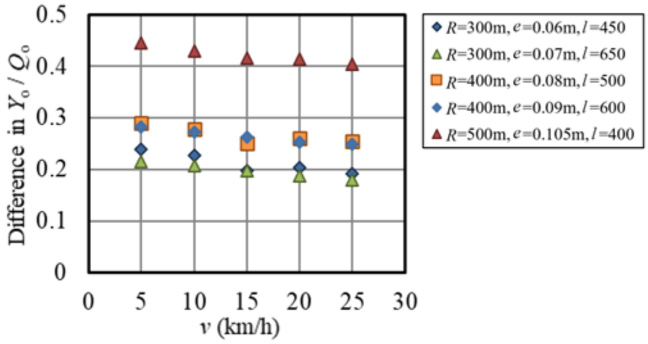

Figure 6: Variation of difference in derailment coefficient as a function of running speed.

Wheel contact points relative to *v* at *w* = 0 m/s and 25.0 m/s are shown in Figure 7. Here, when the wheel contact points reach -36mm, it indicates contact with the flange. Figure 7 shows that at *w* = 0 m/s, regardless of *v*, *e*, or *l*, the contact position shifts away from the flange as *R* increases. On the other hand, at w = 25 m/s, the contact point is approximately -32.5 mm under all conditions except for *R* = 500 m, indicating about -33.5 mm. Although the distance to the flange position is about 2.5 mm ~3.5 mm, crosswinds cause the contact point to move closer to the flange. Figure 8 shows the difference in contact point between *w* = 0 m/s and *w* = 25.0 m/s. In Figure 8, regardless of *v*, *e*, or *l*, the difference in contact point increases as *R* increases.

Based on the above, it was confirmed that under track conditions where the estimated derailment coefficient ratio barely exceeds 1.2, applying crosswinds to a vehicle running through a curve increases the derailment coefficient compared to non-wind conditions. Moreover, the wheel contact point shifts closer to the flange position, increasing the risk of flange climb derailment. Therefore, even on curved sections without anti-derailment guards where the estimated derailment coefficient ratio exceeds 1.2, installing anti-derailment guard is important in environments where strong crosswinds occur. Future research will focus on determining the threshold for the estimated derailment coefficient ratio at which crosswinds do not cause flange climb derailment.

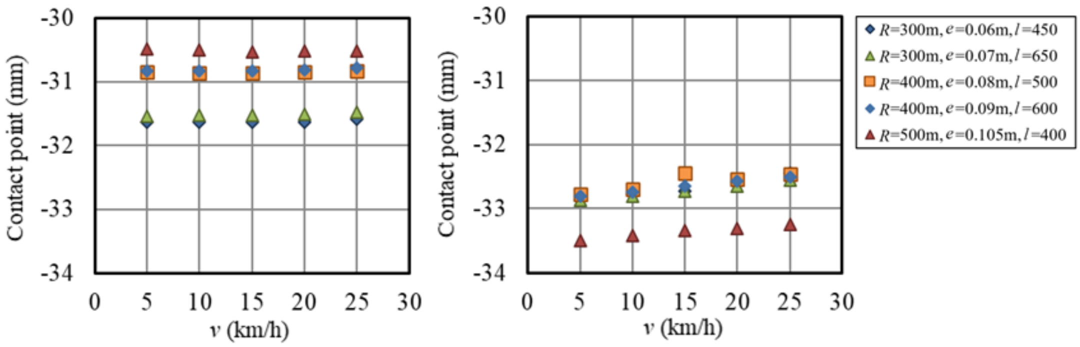

(a) $w = 0$ m/s (b) $w = 25.0$ m/s

Figure 7: Variation of contact point as a function of running speed and wind speed.

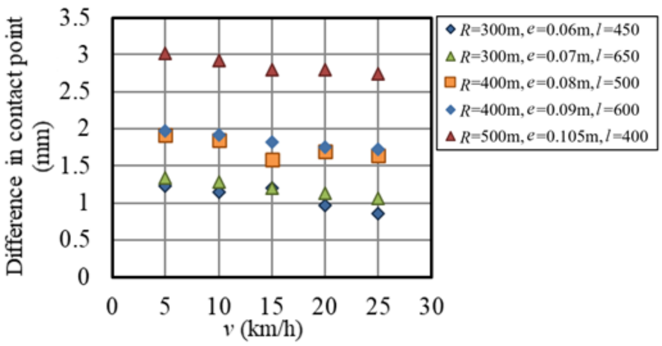

Figure 8: Variation of difference in contact point as a function of running speed.

4 Conclusions

We created the MBD model using the multibody analysis software SIMPACK by converting the specifications of a 1/10 scale vehicle model to full-scale vehicle equivalents. The effects of running a vehicle on a curved track section under crosswinds on the risk of flange climb derailment were examined under track conditions where the estimated derailment coefficient ratio barely exceeded 1.2. The results confirmed that the derailment coefficient increased and the wheel contact point shifted closer to the flange position compared to non-wind conditions. This indicates that installing anti-derailment guard is important in environments with strong crosswinds under track conditions where the estimated derailment coefficient ratio barely exceeds 1.2. In the future, we will conduct a detailed analysis to determine the estimated derailment coefficient ratio threshold that excludes the impact of flange climb derailment.

References

[1] H. Takai, M. Uchida, H. Muramatsu, H. Ishida, "Derailment safety evaluation by analytic equations", Quarterly Report of RTRI, 43, 119-124, 2002.

[2] Accident Investigation Committee, "Investigation Report on the Train Derailment and Collision within Nakameguro Station of the Tokyo Metro Hibiya Line", 2000. (In Japanese)
[3] Y. Hibino, H. Kanemoto, K. Nozaki "Influence of crosswind on flange climb derailment", RTRI Report, 29, No. 9, 41-46, 2002. (In Japanese)